Aspects of Multidimensional Upwinding: Time-Dependent Nonlinear Systems, Source Terms, Spherical Geometries and Three-Dimensional Grid Adaptation. *

M.E.Hubbard

The University of Reading, Department of Mathematics,

P.O.Box 220, Whiteknights, Reading, Berkshire, RG6 6AX, U.K.

30th June 1999

^{*}This work has been carried out as part of the Oxford/Reading Institute for Computational Fluid Dynamics and was funded by EPSRC.

Abstract

A number of peripheral aspects relating to the application of multidimensional upwind schemes in new areas are presented, expanding on their current capabilities. In summary: 1) recently developed high order schemes for the scalar advection equation are applied to nonlinear systems of equations, 2) source term decompositions are presented which are appropriate to existing wave models, 3) the tw

1 Introduction

This report has been written to summarise the current state of a number of strands of research associated with the application of multidimensional upwind schemes (see [6] for full details of these methods) to a wider range of problems. It is divided into four short sections:-

- 2. Multidimensional upwinding has now matured to a stage where it is being used in practical situations for the modelling of steady state aerodynamic problems [9]. However, there is still much work to be done for the approximation of time-dependent flows. Advances have been made for the scalar advection equation [4], combining high order schemes with genuinely multidimensional limiting procedures, and here these techniques are applied to nonlinear systems via existing decompositions. It is clear from the results that although the accuracy is improved significantly there is a necessity for the construction of new and improved wave models.
- 3. Source terms prove to be relatively straightforward to include as part of the fluctuation distribution algorithm and, with the exception of the simple wave models, they can be extended simply to be incorporated within system decompositions. The general technique is described here and compared with the commonly used pointwise approach to illustrate the improvement. In the case of simple wave models one possible method of decomposing and discretising the source terms is described, but it is complicated and unclear as to whether it gives any improvement over the much simpler pointwise discretisation.
- 4. In meteorological flows the shallow water equations are often modelled on the sphere. The decomposition stage of the multidimensional upwind algorithm is not straightforward in this situation, but the scalar schemes can be applied on spherical geometries with little difficulty (if conservation is not enforced) and the method is presented here.
- 5. The grid movement algorithm applied successfully in two dimensions in [1] generalises easily to three dimensions and is applied here to simple scalar

2 Time Dependent Nonline r Systems

The extension of the time-dependent fluctuation redistribution schemes of [4] to nonlinear systems of equations is relatively straightforward and follows closely that of the finite element method [10]. Given that the flux balance can be split up into scalar components, the process differs little from the scalar case:

- compute the low and high order element contributions to the grid nodes using the PSI and Lax-Wendroff schemes respectively, then use these to construct the antidiffusive element contributions (AEC's), storing not only the AEC's for each wave in the decomposition (in the form of distribution coefficients and fluctuations) but also the accumulated element contributions (for speed in calculating the appropriate bounds on the updated solution and hence the required limiting factors).
- compute the complete low order update and use this to obtain bounds on the solution at the new time level.
- use these bounds to calculate limiting factors on the antidiffusive element contributions. These bounds are necessarily constructed from the original solution and the overall updates in terms of the conservative variables. This is because it is not possible to convert perturbations in the conservative variables into perturbations of the 'characteristic' variables associated with the individual waves in the decomposition (due either to the presence of source terms in the decomposition or the linear dependence of the components, depending on the type of wave model used). As a consequence, each wave in the decomposition utilises the same limiting factor at a given cell vertex. This may be based solely on one variable (e.g. density for the Euler equations, depth for the shallow water equations) or taken to be a minimum of the limiting factors over a set of independent variables, such as all of the conservative variables (which should minimise the oscillations in the solution).

3 ~~~~~	······	······	······	<i>/////////////////////////////////////</i>	······	·······	······································
{							
] VAZO VVVVVVV	·///	^^^	^^^	······		··········	www.

and right states before the scheme produced unphysical solutions. Note though that this problem could be alleviated to some extent by increasing the diffusive component of the Lax-Wendroff scheme.

The techniques were also applied to the approximate diagonalisation methods, with similar success but an even more significant lack of robustness, mainly due to the fact that the coupling terms inherent in these models destroy the concept of positivity which is used in the construction of the distribution schemes. Unfortunately, due to their singular nature at stagnation points it is not feasible to apply the preconditioned decompositions even in these simple cases.

3 Source Terms

In two dimensions, source terms have been included in the systems of conservation laws which have been modelled, so the equations become

U

which contains a perturbed gradient of the conservative variables, given by

$$\vec{\nabla}\underline{U}^{\delta} = (\underline{U}_x - \mathbf{A})$$

• **Preconditioned decompositions**: the source term is decomposed in the same way as in the characteristic decomposition above except that the preconditioner is introduced into the transformation, so the flux balance again has the form

$$\underline{\Phi} = -S_{\triangle} \sum_{k=1}^{N_w} (\vec{\lambda}^k \cdot \vec{\nabla} W^k + q^k - S_W^k) \underline{r}^k . \tag{3.11}$$

but \underline{r} are now the columns of the matrix $\frac{\partial \underline{U}}{\partial \underline{Q}} \mathbf{P}^{-1} \frac{\partial \underline{Q}}{\partial \underline{W}}$ and $\underline{S}_W = \frac{\partial \underline{W}}{\partial \underline{Q}} \mathbf{P} \frac{\partial \underline{Q}}{\partial \underline{U}} \underline{S}$. Once more, the solution procedure is no different from the homogeneous case with modified fluctuations.

As an example, the shallow water equations with additional terms for modelling bed slope are solved combining the above technique with the hyperbolic/elliptic preconditioned decomposition adapted from that of Mesaros and Roe [12], and described in detail in [8]. The source terms considered here are

$$\underline{S} = \begin{pmatrix} 0 \\ gdh_x \\ gdh_y \end{pmatrix} = \begin{pmatrix} 0 \\ S_X \\ S_Y \end{pmatrix}$$
 (3.12)

where d is depth, h is depth below still water and g is the acceleration due to gravity, and which, when the transformation to characteristic variables is applied, becomes

$$\underline{S}_{W} = \frac{1}{q^{2}d} \begin{pmatrix} -\varepsilon u S_{X} - \varepsilon v S_{Y} \\ -\beta v S_{X} + \beta u S_{Y} \\ \varepsilon F u S_{X} + \varepsilon F v S_{Y} \end{pmatrix}$$

$$(3.13)$$

in subcritical flow and

$$\underline{S}_{W} = \frac{1}{q^{2}d} \begin{pmatrix} -(u+\beta v)S_{X} - (v-\beta u)S_{Y} \\ -(u-\beta v)S_{X} - (v+\beta u)S_{Y} \\ FuS_{X} + FvS_{Y} \end{pmatrix}$$
(3.14)

when the flow is supercritical. As in [8], u and v are the two velocity components, $q = \sqrt{u^2 + v^2}$ is the flow speed, $F = q/\sqrt{gd}$ is the local Froude number,

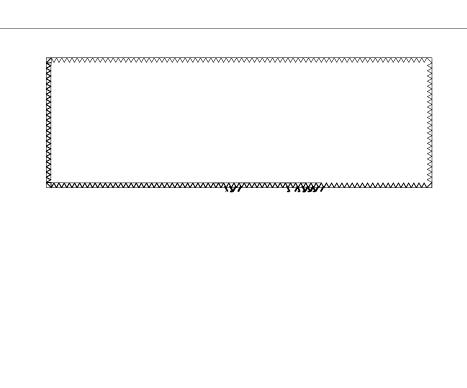
$$\beta = \sqrt{|F^2 - 1|} , \quad \kappa = \max(F, 1) ,$$
 (3.15)

and, in this case, ε is taken to be

$$\varepsilon(F) = \begin{cases} -F^3 + \frac{3}{2}F^2 + \frac{1}{2} & \text{for } 0 \le F \le 1\\ 1 & \text{for } F > 1. \end{cases}$$
 (3.16)

3.1 Results

Results are shown, comparing the upwind distribution of the source terms described above with a simple pointwise evaluation at each node which is added



The subscript \cdot_{∞} represents the freestream flow values 'at infinity' which are used in the application of simple characteristic boundary conditions at inflow and outflow: appropriate Riemann invariants are specified, *cf.* [7].

Each of the sets of results in Figure 3.2 shows an improvement when the upwind discretisation of the source term is used. Discharge is supposed to remain constant throughout the channel for steady state flows. The small discrepancies seen in the supercritical case are there simply due to linearisation errors and could be removed with a little extra effort in the linearisation of the source term to achieve an exact balance with the linearised flux gradients. In the transcritical flow case, the difference from the exact one-dimensional solution appears to come from the application of the boundary conditions in two dimensions, and is visible in results obtained from other forms of numerical scheme.

4 ultidimension l Upwinding on the Sphere

The first question which needs to be addressed here is whether the schemes should be applied in a three-dimensional Cartesian coordinate system or a spherical polar coordinate system. The former has been chosen here because it avoids the singularity which appears at the poles in the latter. Since the schemes are applied on unstructured triangular grids there is no problem with grid singularities, which occur in many existing structured codes. The big advantage of this approach is that the advection is treated in the same way, regardless of position on the surface of the sphere and direction of travel.

Ideally, the underlying scheme would be based on the two-dimensional multidimensional upwind schemes, but applied on a curved surface. Unfortunately, since the divergence theorem can no longer be applied in the conservation argument, the resulting scheme is not conservative because internal cancellation can no longer be guaranteed. However, in the scalar case it should be simple to construct a conservative three-dimensional scheme on a prismatic grid over the surface of the sphere in which the solution is constrained to be constant perpendicular to the curved surface. For the momen

space so, given a two-dimensional set of orthogonal coordinates ξ and η in the plane of the triangle on the surface, the fluctuation can be defined by

$$\phi = \iint_{\Delta} \vec{\nabla}_{\xi\eta} \cdot (f^{\xi}, g^{\eta}) \, d\xi \, d\eta , \qquad (4.1)$$

where f and g are both functions of u. This can be approximated by

$$\tilde{\phi} = -S_{\triangle} \tilde{\vec{\lambda}}_{\xi\eta} \cdot \vec{\nabla}_{\xi\eta} u \approx \oint_{\partial \triangle} (f^{\xi}, g^{\eta}) \cdot d\vec{n}_{\xi\eta} . \tag{4.2}$$

Alternatively, in keeping with the three-dimensional coordinate system, one can take

$$\tilde{\phi} = \sum_{k=1}^{N_e} (\tilde{f}, \tilde{g}, \tilde{h}) \cdot \vec{n}_k \tag{4.3}$$

in which \vec{n}_k is a three-dimensional 'outward' normal to the edge of the triangle whose direction is tangent to the surface at the midpoint of the edge and whose component in the plane of the cell has the same length as the corresponding edge. Thus \vec{n}_k is not in the ξ - η coordinate plane and the approximation cannot be exact, even under the assumptions of linearly varying u and constant advection. However, both of the above approximations are consistent and the distribution coefficients can be calculated as for the two-dimensional scheme (since everything is carried out locally on the triangle) and the same overall update used.

4.1 Results

Figure 4.1 shows the initial conditions (and the exact solution after one revolution) for the advection of a cosine bell around a great circle of a sphere proposed in [13]. Figures 4.2 and 4.3 show the numerical solution on the coarse grid illustrated (1357 nodes, 2710 cells) after one revolution, respectively around the equator and across the poles. The scheme used is in fact the implicit consistent finite element version of the PSI scheme [11] with flux-corrected transport applied to ensure monotonicity and the solutions look reasonably good despite the lack of conservation. Importantly there is little difference between the solutions obtained for the advection over the poles and around the equator, and no special treatment of the poles has been necessary.

Figure 4.1: The initial conditions for advection on the sphere.

Figure 4.2: The solution after one revolution around the equator for advection on the sphere.

Figure 4.3: The solution after one revolution across the poles for advection on the sphere.

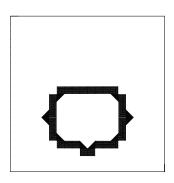
5 Three-Dimension l Grid Ad pt tion

The simple grid movemen

3) fix the grid and run the time-stepping algorithm to convergence using the solution from step 2) as initial conditions.

5.1 Results

Results are shown for a simple test case of advection through a cube with dimensions $[-1,0] \times [0,1] \times [0,1]$, as described in [5]. The boundary conditions are zero everywhere at inflo



techniques for improving accuracy and efficiency, such as implicit time-stepping and grid adaptation through both refinement and movement. Viscous flow models

- [2] M.E.Hubbard, 'Multidimensional upwinding and grid adaptation for conservation laws', PhD Thesis, The University of Reading, 1996.
- [3] M.E.Hubbard and M.J.Baines, 'Conservative multidimensional upwinding for the steady two dimensional shallow water equations', J. Comput. Phys., 138:419-448, 1997.
- [4] M.E.Hubbard and P.L.Roe, 'Compact high-resolution algorithms for timedependent adv

- [12] L.M.Mesaros and P.L.Roe, 'Multidimensional fluctuation splitting schemes based on decomposition methods', AIAA Paper 95-1699, 1995.
- [13] D.L.Williamson, J.B.Drake, J.J.Hack, R.Jakob and P.N.Swarztrauber, 'A standard test set for numerical approximations to the shallow water equations in spherical geometry', *J. Comput. Phys.*, **102**:211–224,AIAAnt1"2r2.